Image Information Restoration Based on Long-Range Correlation

David Zhang, *Senior Member, IEEE*, and Zhou Wang

***Abstract*—A new class of image information-restoration algorithms virtually different from traditional techniques are proposed. In comparison with other approaches, our methods not only use the information in local areas, but also that in the remote regions in the image. The methods originate from the idea that *there exists abundant long-range correlation within natural images and the human vision systems composed of our eyes and brains can sufficiently utilize such types of information redundancy to implement the functions of image interpretation, representation, restoration, enhancement, and error concealment*. Our general approach can be summarized as five basic steps: fetching, searching, matching, competing, and recovering. The experimental results on several practical applications show that our methods perform substantially better than many other state-of-the-art methods.**

***Index Terms*—Block-based image coding, error concealment, image information restoration, impulse noise removal, long-range correlation.**

I. Introduction

WE would like to begin this paper by performing a simple test. Let us look at two pictures that are shown as Fig. 1(a) and (b). It can be observed that the middle block regions of these two pictures are missing. This raises the questions: "What should be in the lost blocks? Can you give a good guess?" When we asked dozens of people these questions, all of them gave almost the same answers. They found it difficult to guess the missing block in the first picture, but were able to imagine the missing block in the second picture. People were surprised when we told them that the lost blocks in these two pictures are exactly the same block removed from the same standard image. The only difference is that in Fig. 1(a), the block is very closely observed, while in Fig. 1(b), the block is observed from a remote position so that a larger background region can also be seen. Why people can give much better estimation of the lost block from the second picture than from the first picture? In our opinion, at least two conclusions can be drawn from this test. First, there exists abundant long-range correlation within natural images which can be viewed as a special kind of information redundancy. Second, the human vision systems composed of our eyes and brains can and do use such correlations to interpret and restore image information.

Manuscript received August 15, 1999; revised September 3, 2001. This paper was recommended by Associate Editor D. Liu.

D. Zhang is with the Center for Multimedia Signal Processing and Department of Computing, Hong Kong Polytechnic University, Hung Hom, Kowloon, Hong Kong (e-mail: csdzhang@comp.polyu.edu.hk).

Z. Wang is with the Laboratory for Image and Video Engineering (LIVE), Department of Electrical and Computer Engineering, The University of Texas at Austin, Austin, TX 78712-1084 USA (e-mail: zhouwang@ieee.org).

Publisher Item Identifier S 1051-8215(02)05264-3.

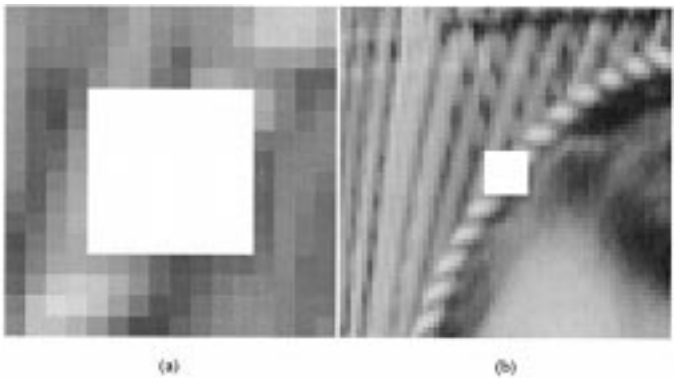

Fig. 1. The same lost block under different scales of backgrounds. (a) Local region background. (b) Large region background observed from a remote position.

Now let us come to the traditional image-restoration and image-enhancement techniques. Basically, they can be classified in three categories: 1) pixel point processing method; 2) pixel group processing method; and 3) frequency-domain method. In the first method, the gray level of each pixel in the input image is modified to a new value, often by a mathematical or logical relationship, and placed in the output image at the same spatial location. All pixels are handled individually [1]. Typical examples are histogram sliding and stretching algorithms and binary contrast enhancement approaches. The second method, namely pixel group processing, operates on a group of input pixels surrounding a center pixel, resulting in the output center pixel value. Examples are low- and high-pass linear spatial filters, gradient operator-based edge detection/enhancement algorithms, and the median-based filters. In the third method, a frequency transformation decomposes an image from its spatial-domain form of brightness, into a frequency-domain form of fundamental frequency components [1]. The real image-restoration and image-enhancement processing is conducted by modifying the frequency components. To reconstruct the image, an inverse frequency transformation converts an image from its frequency domain form back to a spatial form. The most common transform is the Fourier transform. There are also other transforms, such as the Hadamard, Harr, slant, Karhunen-Loeve, sine, and cosine transforms [1].

The limitation of traditional image restoration approaches is obvious because whenever they belong to one of the three methods mentioned above, only the pixels in a very limited local region are directly used as the information source to create the new value of a pixel. Although the frequency transformation method can, in some extent, make use of the information, such as the magnitude of the energy on a certain frequency,

of a large area, the information of remote regions are used only statistically but not directly. Consequently, traditional methods are impossible to simulate the human vision systems in utilizing long-range correlation in the images. In contrast, our new algorithms to be presented in this paper are just based on the employment of such long-range information redundancy.

It should be mentioned that in Jacquin's fractal block coding (FBC) algorithm [2], [3], some kinds of block-wise self-similarities had been used for the compression of images. The concept of self-similar in the FBC algorithm is very flexible. In some cases, it means an image block is very similar to some part of itself. In some other cases, it can also mean a small image block is similar to a remote larger block in the same image. It can be shown that this second kind of block-wise similarity is actually a special form of the long-range correlation discussed in this paper. Another major contribution of Jacquin is that he introduced a practical way to find long-range block-wise similarities. Our approaches use similar ways to find long-range correlation in images. However, our algorithm has many differences in comparison with FBC. First, the goal of our method is for information restoration rather than image compression. The long-range correlation between image pieces is used for recovering damaged image pixels, instead of removing redundancy to compress the image. Second, our method cannot be called *fractal* because the word "fractal" in "fractal image coding" means self-similarity at different scales, while we are trying to use long-range similarities at the same scale.

This paper is organized as follows. In the next section, a general approach of our image restoration algorithm using long-range correlation is presented. Three real applications are provided in Section III. The experimental results are also shown in this section. In Section IV, we discuss many possible extensions and improvements of our method. Finally, some concluding remarks are given in Section V.

II. General Approach

Before the application of our general image-restoration approach, we should make two assumptions. First, only some of the pixels in the image are bad (lost or damaged) while the other pixels are good (uncontaminated, the same as those in the original image). Second, we have known which pixels are good and which pixels are bad. In case we do not have this kind of information, an error or noise detection algorithm should be applied first.

A digital gray scale image $\boldsymbol{x}$ with M pixels can be denoted as a vector $\boldsymbol{x} = (x_1, x_2, \ldots, x_M)$. For convenience, a 1-D model is used in this paper. Nevertheless, the algorithms presented below are also applicable or can be easily adapted to 2-D or higher dimensional cases. Let $\boldsymbol{x}$ and $\boldsymbol{x}^{(\mathrm{new})}$ be the damaged image and the restored image, respectively. Since we know which pixels in the image are good, it is easy to give each pixel x_i $(i = 1, 2, \ldots, M)$ a binary flag f_i, indicating whether it is bad, i.e., $f_i = 0$ means x_i is good and $f_i = 1$ means x_i is bad. The goal of our image restoration algorithm is to give each bad pixel with $f_i = 1$ a new value $x_i^{(\mathrm{new})}$ that can comply well with our visual sense.

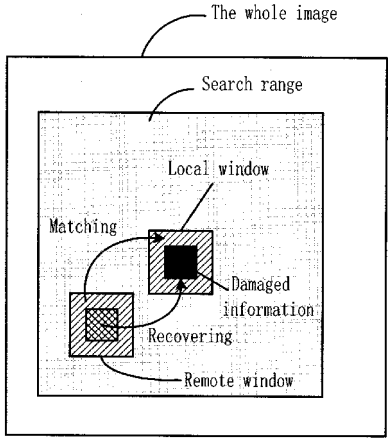

Fig. 2. Demonstration of the general approach.

Our general image-restoration approach is composed of five basic steps. For the ease of description, a demonstration graph is provided in Fig. 2. The five steps are given as follows.

1) *Fetching*: Extract a window $\boldsymbol{l}$ with N pixels from the image which is called a local window (see Fig. 2). We have $\boldsymbol{l} = (l_1, l_2, \ldots, l_N)$. This window may be a square, rectangle, triangle, or any other shape. The only restriction is that all the pixels are contiguously connected. For each pixel l_i $(i = 1, 2, \ldots, N)$ in this local window $\boldsymbol{l}$, we can get its corresponding flag value f_i^l. The set of pixels with $f_i^l = 1$ is shown as the damaged information in the local window (see Fig. 2).
2) *Searching*: Search for another window $\boldsymbol{r}$ in the image which is of exactly the same shape and the same size as the local window $\boldsymbol{l}$. We call $\boldsymbol{r}$ a remote window (see Fig. 2) and have $\boldsymbol{r} = (r_1, r_2, \ldots, r_N)$. The flag value of each pixel r_i in window $\boldsymbol{r}$ is denoted as f_i^r. Since the $\boldsymbol{l}$ and $\boldsymbol{r}$ are of the same shape and size, we can find an indexing method that makes every pixel in $\boldsymbol{l}$ correspond to a unique pixel at the same position in $\boldsymbol{r}$ and vice versa. Sometimes, we restrict the searching procedure to be conducted in a region not very far from the local window. We call such a region the search range (see Fig. 2). Obviously, if a full search is conducted in the search range, we can find many candidate remote windows. In the next two steps, we will try to find out which is the best for our needs.
3) *Matching*: Try to match the remote window $\boldsymbol{r}$ to the local window $\boldsymbol{l}$. The matching method is determined by a 1-D luminance transformation function v that transforms every r_i in $\boldsymbol{r}$ to $v(r_i)$. There are many possible matching methods. The simplest form is direct matching, where we use $v(z) = z$ (where z denotes a real number) as the luminance transformation. Other practical luminance transformations include the p-order polynomial functions

$$v(z) = a_0 + a_1 z + \cdots a_p z^p, \quad (p \geq 1) \tag{1}$$

where $a_0, a_1, \ldots,$ and a_n are the polynomial coefficients. The pixel pairs in the two windows can be classified into three categories. In the first category, the corresponding pixels in $\boldsymbol{r}$ and $\boldsymbol{l}$ are good ($f_i^l = 0$ and $f_i^r = 0$). In

the second category, the pixel in $\boldsymbol{r}$ is good, but its corresponding pixel in $\boldsymbol{l}$ is bad ($f_i^l = 1$ and $f_i^r = 0$). In the last category, the pixel in $\boldsymbol{r}$ is bad irrespective of whether its corresponding pixel in $\boldsymbol{l}$ is good or not ($f_i^r = 1, f_i^l = 0$ or $f_i^l = 1$). The pixels in the first category compose the matching part of the window. The number of pixels in this category is

$$n_M = \sum_{i=1}^{N} [1 - f_i^r] \cdot [1 - f_i^l]. \tag{2}$$

Actually, only the pixels in this part will be used in the matching procedure. The matching result is evaluated by the mean-squared error of the matching part (MSE_M) between the transformed $\boldsymbol{r}$ window and the $\boldsymbol{l}$ window

$$\mathrm{MSE}_M = \frac{1}{n_M} \sum_{i=1}^{N} [1 - f_i^r] \cdot [1 - f_i^l] \cdot [l_i - v(r_i)]^2. \tag{3}$$

Of course, we want the MSE_M to be as small as possible. In practice, we can use the condition of minimal MSE_M to calculate the parameters in the luminance transformation v. For example, if we use one of the polynomial functions of (1) as the luminance transformation function, then the parameters can be obtained by solving the following set of equations:

$$\begin{cases} \partial \mathrm{MSE}_M / \partial a_0 = 0 \\ \partial \mathrm{MSE}_M / \partial a_1 = 0 \\ \quad \vdots \\ \partial \mathrm{MSE}_M / \partial a_p = 0. \end{cases} \tag{4}$$

For the one-order case, the solution is given as in (5), shown at the bottom of the page.

4) *Competing*: All the candidate remote windows compete for the best match for the local window. Each candidate remote window in the search range will result in its corresponding MSE_M. An obvious effective standard for the selection of remote windows is to choose the one with the least MSE_M. This remote window then becomes the winner. In Section IV of this paper, we will discuss the possibility of using more complex standards by combining other parameters such as the distance between the local and remote windows.
5) *Recovering*: Recover the damaged pixels in the local window using the good pixels in the transformed remote window. Suppose we have the winning remote window $\boldsymbol{r}$ and its related matching transformation function v. Because the remote window and the local window are very well matched, some bad pixels ($f_i^l = 1$) in $\boldsymbol{l}$ can be recovered by using their corresponding good pixels ($f_i^r = 0$) in $\boldsymbol{r}$. This is why we call the set of the pixels in the second category of the windows ($f_i^l = 1$ and $f_i^r = 0$) the recovering part. For a certain pixel in this part, the new pixel value is

$$l_i^{(\mathrm{new})} = \begin{cases} v(r_i), & \text{if } f_i^l = 1 \quad \text{and} \quad f_i^r = 0 \\ l_i, & \text{otherwise.} \end{cases} \tag{6}$$

Finally, we copy the renewed local window back into its corresponding position in the recovered image and modify the flag values of the recovered pixels from 1 to 0.

By applying the five steps above, some bad pixels ($f_i^l = 1$ and $f_i^r = 0$) in the contaminated image are recovered. The restoration of the whole image needs to apply these steps many times until the flags of all the pixels in the image are all 0.

We have proposed the general framework for image restoration using long-range correlation. In real applications, such a framework should be adapted to the practical requirements. For example, in some circumstances, the contaminated pixels may not be totally damaged. Their values can be viewed as the combination of their original values and later mixed noises. In such cases, the matching, competing, and recovering algorithms should be modified accordingly.

III. Applications

A. Error Concealment for Block-Based Image-Coding Systems

Recently, many image-coding algorithms have been developed to reduce the bit rate for digital image and video representation and transmission. Among them, block-based techniques have proved to be the most practical and are adopted by most existing image and video compression standards [4]–[6]. Since real-world communication channels are not error free, the coded data transmitted on them may be corrupted. Block-based image-coding systems are vulnerable to transmission impairment. Loss of a single bit often results in loss of a whole block and may cause consecutive block losses. Many error-concealment methods have been proposed [7]–[12], which are aimed at masking the effect of these missing blocks to create subjectively acceptable images.

We call our error concealment method the best neighborhood matching (BNM) algorithm. In our experiments, only 8×8 sized block losses are considered. The reason to choose such a size is that it is the size frequently used by a lot of proposed image and video coding techniques. The lost 8×8 blocks are recovered one by one. The sizes of the local window $\boldsymbol{l}$ and the

$$\begin{cases} a_1 = \dfrac{n_M \cdot \sum_{i=1}^{N} (1 - f_i^r)(1 - f_i^l) \cdot r_i \cdot l_i - \left[\sum_{i=1}^{N} (1 - f_i^r)(1 - f_i^l) \cdot r_i\right] \cdot \left[\sum_{i=1}^{N} (1 - f_i^r)(1 - f_i^l) \cdot l_i\right]}{n_M \cdot \sum_{i=1}^{N} (1 - f_i^r)(1 - f_i^l) \cdot r_i^2 - \left[\sum_{i=1}^{N} (1 - f_i^r)(1 - f_i^l) \cdot r_i\right]^2} \\ a_0 = \dfrac{1}{n_M} \left[\sum_{i=1}^{N} (1 - f_i^r)(1 - f_i^l) \cdot l_i - a_1 \cdot \sum_{i=1}^{N} (1 - f_i^r)(1 - f_i^l) \cdot r_i\right] \end{cases} \tag{5}$$

Fig. 3. Top left: Damaged image "Barb" with isolated block losses and with block loss rate of 10%, $\mathrm{PSNR} = 16.43$ dB. Top right: Reconstructed image "Barb" by dc concealment, $\mathrm{PSNR} = 29.95$ dB. Botom left: Reconstructed image "Barb" using one-order BNM algorithm, $\mathrm{PSNR} = 37.08$ dB. Bottom right: Original image "Barb."

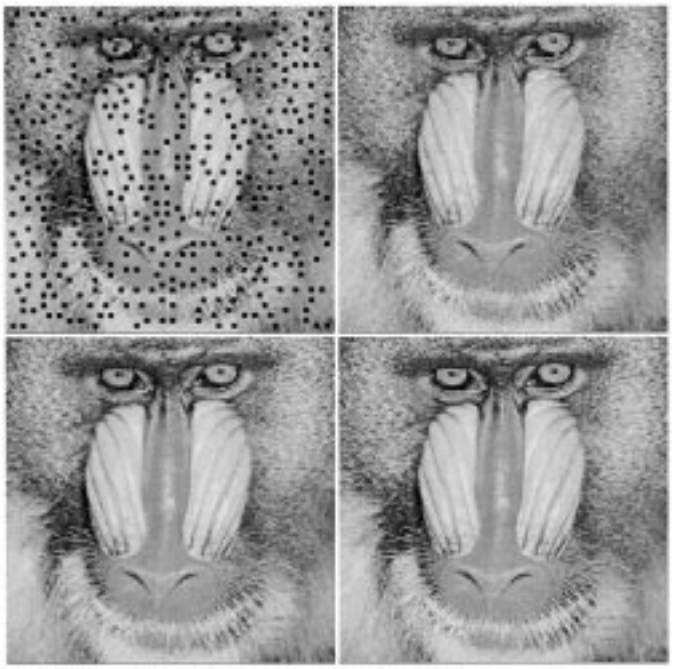

Fig. 4. Top left: Damaged image "Baboon" with isolated block losses and with block loss rate of 10%, $\mathrm{PSNR} = 15.48$ dB. Top right: Reconstructed image "Baboon" by dc concealment, $\mathrm{PSNR} = 28.89$ dB. Bottom left: Reconstructed image "Baboon" using one-order BNM algorithm, $\mathrm{PSNR} = 29.03$ dB. Bottom right: Original image "Baboon."

remote window $\boldsymbol{r}$ are fixed to be 10×10. The candidate remote windows are selected from an 80×80 square region (what we referred to as the search range) with the local window located at its center. Another restriction on a candidate remote window is that it must be a good block itself. In other words, all the pixels in it are good. We put the 8×8 lost block at the center of the local window, thus the matching part of the local window is a one pixel wide boundary around the lost block. The remote window whose boundary pixels match the neighborhood of a lost block the best, becomes the winning remote window. This is why we call our method the BNM algorithm. For luminance transformations, the direct matching and one-, two-, and three-order polynomial matching functions are tried, where the best coefficients $a_0, a_1, \ldots, a_n$ of the n-order polynomial functions are obtained under the condition of least MSE_M as given above. Through experiments, we find that the one-order polynomial function is the best for luminance transformation. Nevertheless, the direct matching function can get similar restoration results within much less time. In general, higher polynomial orders, such as the two- or three-order, lead to smaller MSE_M. However, this does not mean their restoration results are always better than those obtained by lower order functions. The reason is that it may falsely result in absurd recovery, i.e., two blocks that are not similar may become very similar through a high-order luminance-matching function. In other words, the lower order functions, although not good at function approximation, are more robust and have better generalization ability.

Two cases of block losses are considered. In the first case, the lost blocks are restricted to be isolated, i.e., all of their 8 surrounding blocks are good blocks. In the other case, no restriction is applied, so that some adjacent missing blocks may be connected into big lost regions. For the first case, we can use our approach directly to recover the lost blocks one by one. For the second case, a complete boundary for some missing blocks may not be available. Two modifications are used to solve this problem. First, we exclude the missing pixels in the one pixel wide boundary of a missing block from the matching part of the window. Thus, the matching test is applied on the remaining good boundary pixels only. Second, we recover the damaged image through a progressive procedure which is composed of several steps. The missing blocks recovered in the current step are considered as good blocks in the subsequent steps. By using such a progressive procedure, the more a lost block is surrounded by good boundary pixels, the earlier it is recovered.

The simulations on both the cases show that our algorithm can get very good restoration results in terms of both subjective and objective evaluations. Figs. 3 and 4 give the restoration result of two standard images with 10% isolated block losses. Fig. 5 shows some enlarged sample regions for sharp edge areas, stripe areas, texture areas, and very complex areas, respectively. The visual quality of the recovered blocks are very good even when the areas contain a lot of detailed information that is very difficult to be handled by other approaches. For object evaluation, a peak signal-to-noise ratio (PSNR) is used as the criterion, which is defined as

$$\mathrm{PSNR} = 10 \log_{10} \frac{255^2}{\frac{1}{M} \sum_{i=1}^{M} (o_i - t_i)^2} \tag{7}$$

where M is the number of pixels in the image, and o_i and t_i are the i-th pixel values in the original and the test images, respectively. In Table I, we present the restoration results for image

(a)

(b)

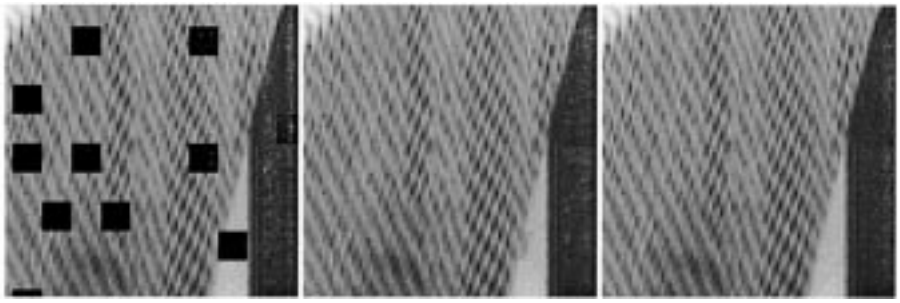

(c)

(d)

Fig. 5. Enlarged sample regions for: (a) sharp edge area; (b) stripe area; (c) texture area; and (d) very complex areas. (Left: Damaged. Middle: Restored. Right: Original.)

TABLE I
PSNR PERFORMANCE FOR DIFFERENT ERROR CONCEALMENT METHODS WITH BLOCK LOSS RATES RANGING FROM 2.5% TO 15.0%

Error Concealment Algorithm	Block Loss Rate					
	2.5 %	5.0 %	7.5 %	10.0 %	12.5 %	15.0 %
without concealment	22.8 dB	19.4 dB	17.7 dB	16.4 dB	15.3 dB	14.6 dB
dc concealment	36.6 dB	32.9 dB	31.4 dB	30.0 dB	29.2 dB	28.0 dB
direct BNM	41.1 dB	39.0 dB	36.3 dB	35.7 dB	33.6 dB	32.3 dB
1-order BNM	41.8 dB	39.6 dB	37.6 dB	37.1 dB	35.0 dB	33.2 dB

"Barb" using direct BNM and one-order BNM algorithms, respectively. For comparison, we also include the restoration results of the dc concealment method in Figs. 3 and 4 and Table I. The dc concealment method simply fills the lost block with a

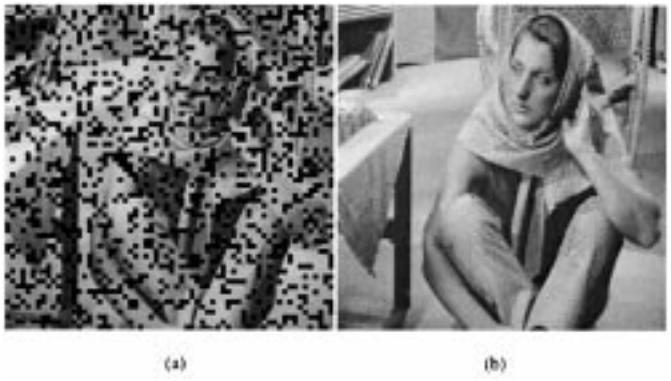

Fig. 6. (a) Damaged image "Barb" with contiguous block losses and with a high block loss rate of 30%, $\mathrm{PSNR} = 11.79$ dB. (b) Reconstructed image "Barb" using BNM algorithm, $\mathrm{PSNR} = 29.13$ dB.

uniform gray value equal to the average gray level of its eight surrounding blocks. The dc concealment algorithm can improve PSNR by a magnitude of about 13–14 dB, while those for direct and one-order BNM algorithms are about 18–20 and 19–21 dB, respectively. The PSNR performance of the one-order BNM algorithm for image "Barb" with a block loss rate of 10% is 37.08 dB, which is a significant improvement over 31.2 dB of Sun's scheme [8], 32 dB of HCIE scheme [10], and 34.5 dB of Lee *et al.*'s fuzzy logic scheme [10]. Similar results are also obtained on other test images with different lost block rates. In Fig. 6, the restoration result of "Barb" with very highly corrupted 30% contiguous block losses is provided. Even though some lost blocks are connected into large black regions, we still obtain good restoration in most of the regions.

B. Impulse Noise Removal

Images are often contaminated by impulse noise due to errors generated in noisy sensors and communication channels. It is important to eliminate noise in the images before some subsequent processing, such as edge detection, image segmentation and object recognition. A large variety of filtering algorithms have been proposed to perform an effective noise cancellation while preserving the image structure [13]–[17]. Since impulse noise only contaminates a proportion of the pixels in the images and its value is generally independent of the strength of the image signal, our general approach described above is very suitable and can be easily adapted to eliminate such noises [18].

Before the application of our noise-cancellation algorithm, however, a noise detector is used to give each pixel a binary flag value, indicating whether it is an impulse pixel. In [17], we introduced an impulse-detection algorithm before the application of a polynomial approximation approach. The impulse detector is an improved iterative version of Sun and Neuvo's switch I method [15] and is based on two assumptions on the image: 1) a noise-free image should be locally smooth varying and is separated by edges [15] and 2) a noise pixel takes a gray value substantially larger than or smaller than those of its neighbors. Experiments show that our detector is very good at detecting impulsive noises in the images, especially when the images are very highly contaminated. We use it here to generate the binary flags.

During the noise removal procedure, the impulses are eliminated one by one. The local window is of size 7×7 centered about the impulse pixel. A candidate remote window must satisfy the following conditions: 1) it is not the same as the local window; 2) it must be completely covered by the 21×21 window (the search range) centered about the impulse; and 3) its center pixel is good. Similar to those in the error concealment method, we still use MSE_M to evaluate the matching result and the one-order polynomial for the luminance transformation, whose coefficients are obtained by (5).

Two cases of noise distributions are considered. In the first case, the values of the corrupted pixels are equal to the maximum or minimum of the allowed dynamic range with equal probability. This kind of noise is commonly referred to as salt-pepper noise. In the other case, the corrupted pixel values are uniformly distributed between the minimum and maximum allowed dynamic range. For 8-bits/pixel (bpp) gray-level images, the noise luminance of the first case corresponds to a fixed value of 0 or 255 with equal probability, while that of the second case corresponds to a random value uniformly distributed between 0 and 255.

In Fig. 7, we give some enlarged areas of our test images to show how the proposed algorithm performs on different kinds of image details corrupted with fixed-valued and random-valued impulsive noises. The visual qualities of the restored images are relatively good considering the abundance of image details and the high noise probabilities. Table II compares our method with other well-known methods in PSNR for the standard image "Lena" corrupted by 20% fixed-valued and random-valued impulses. For fixed-valued noise, our algorithm provides significant improvement over all the other approaches, while for random-valued noise, only Abreu *et al.*'s approach with inside training set [16] is close to our algorithm. In Table III, we show the filtering results for image "Lena" corrupted by random-valued impulse noise with various probabilities ranging from 10% to 30%. The results of Abreu *et al.*'s approach are also given [16]. In most cases, the performance of the proposed algorithm is close to the best result of Abreu *et al.*'s approaches. Notice that our algorithm does not include any training procedure. When the noise probability is high, the restoration results may be further improved simply by iteratively applying the proposed algorithm. In the last row of Table III, we list the PSNR performance after two iterations.

C. Reduction of Blocking Effect

The "blocking effect" is one of the major disadvantages of block-based image-coding techniques. There are two general approaches to reduce blocking effects: overlapping the blocks during encoding [19], [20] and post-processing after decoding [19], [21]–[25]. Our method belongs to the second approach.

The reduction of blocking effect is much different from the above two applications because no pixel in the image is totally damaged. In other words, the pixel values near block boundaries also contain some useful information that should not be eliminated. The goal of the algorithm is just to modify these pixel values to reduce the discontinuity across the two adjacent blocks.

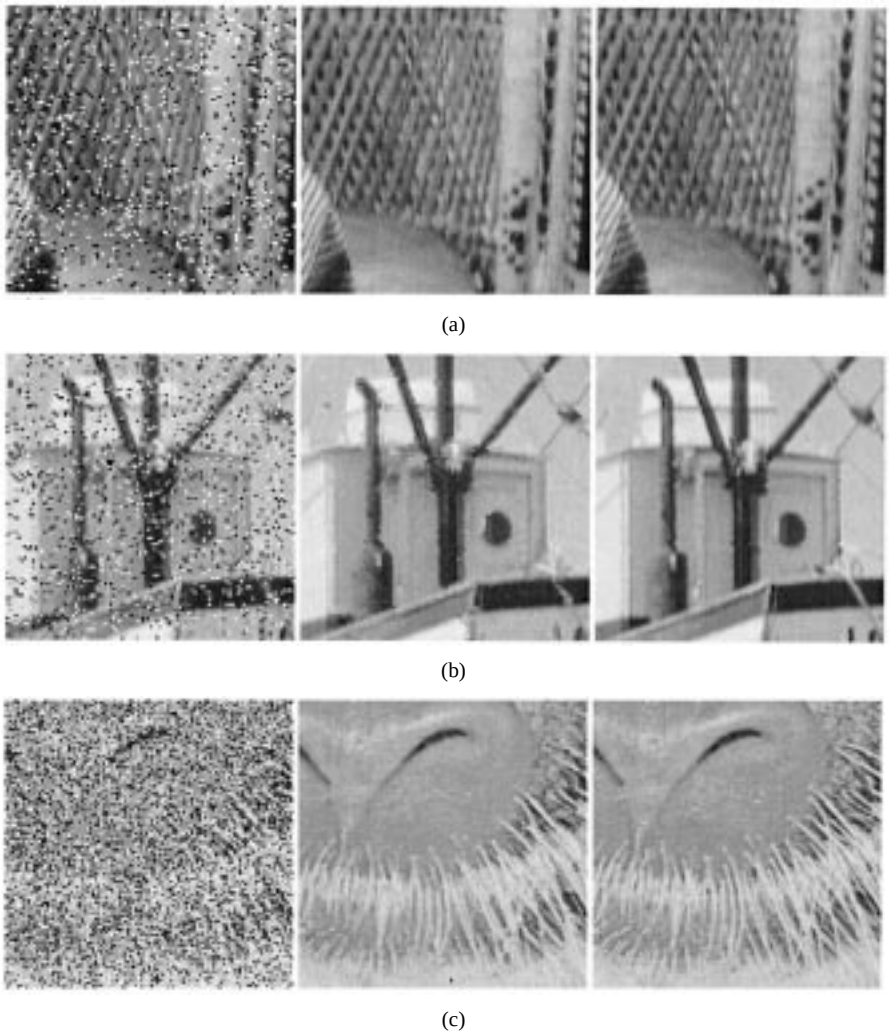

Fig. 7. Impulse noise restoration performance. (a) Enlarged area from image "Barb" corrupted by 10% fixed-valued impulse noise. (b) Enlarged area from image "Boats" corrupted by 20% random-valued impulse noise. (c) Enlarged area from image "Baboon" corrupted by 30% fixed-valued impulse noise. Left: Corrupted images. Middle: Restored images. Right: Original image areas.

TABLE II
COMPARATIVE RESTORATION RESULTS IN PSNR FOR 20% IMPULSE NOISE FOR IMAGE "LENA". FOR FIXED-VALUED IMPULSE NOISE, IMPULSES TAKE ON ONLY THE VALUES 0 OR 255 WITH EQUAL PROBABILITY. FOR RANDOM-VALUED IMPULSE NOISE, IMPULSE VALUES ARE UNIFORMLY DISTRIBUTED BETWEEN 0 AND 255

Filtering Algorithm	Fixed-valued Impulses	Random-valued Impulses
Median filter (3×3)	28.57 dB	29.76 dB
Median filter (5×5)	28.78 dB	28.59 dB
Median filter with adaptive length[1] [13]	30.57 dB	31.18 dB
Rank conditioned rank selection filter[1] [14]	31.36 dB	30.78 dB
Sun and Neuvo, Switch I median filter[1] [15]	31.97 dB	31.34 dB
Sun and Neuvo, Switch II median filter[1] [15]	29.96 dB	32.04 dB
Abreu et al. (M=2, no training)[1] [16]	33.47 dB	32.47 dB
Abreu et al. (M=1296, outside training set)[1] [16]	34.65 dB	32.95 dB
Abreu et al. (M=1296, inside training set)[1] [16]	35.70 dB	33.37 dB
Our long-range correlation method [18]	36.95 dB	33.43 dB
Combine our method with fuzzy techniques [26]	36.47 dB	33.78 dB

[1] See [16] for more details with regard to methods and parameter selections.

Suppose the image is partitioned into 8×8 blocks and encoded separately. Then after decoding, all the blocking effects appear on the pixels near the boundaries of these 8×8 blocks. Our algorithm is based on the assumption that the pixels within the same block are of good continuity. Such good continuity is used to recover the discontinuity across block boundaries. Our algorithm is first applied horizontally to recover vertical boundaries and then applied vertically

TABLE III
COMPARATIVE FILTERING RESULTS IN PSNR FOR IMAGE "LENA" CORRUPTED WITH VARIOUS PERCENTAGES OF RANDOM-VALUED IMPULSE NOISE

Filtering Algorithm	Percentage of Random-valued Impulse Noise				
	10%	15%	20%	25%	30%
Abreu et al. (M=2, no training)[1] [16]	35.18 dB	33.94 dB	32.47 dB	31.18 dB	29.87 dB
Abreu et al. (M=1296, inside training set)[1] [16]	36.02 dB	34.44 dB	33.37 dB	31.77 dB	30.49 dB
Abreu et al. (M=1296, outside training set)[1] [16]	36.64 dB	34.72 dB	32.95 dB	31.52 dB	29.99 dB
Our long-range correlation method, 1 iteration	36.69 dB	34.83 dB	33.43 dB	31.76 dB	30.01 dB
Our long-range correlation method, 2 iterations	36.11 dB	34.71 dB	33.75 dB	32.54 dB	31.50 dB

[1] See [16] for more details with regard to methods and parameter selections.

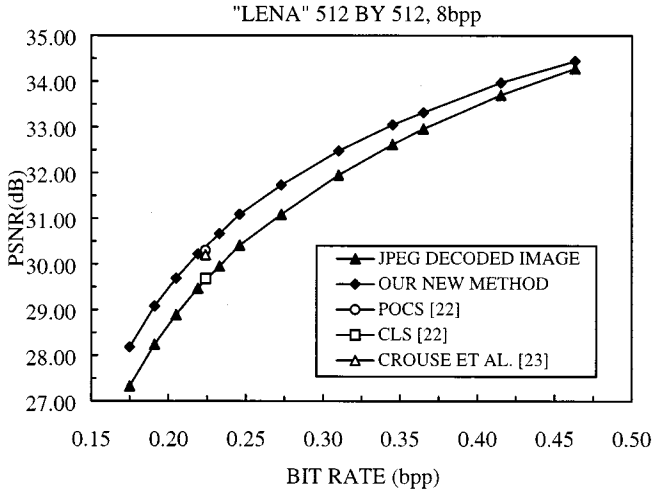

Fig. 8. Post-processing results for JPEG-decoded image "Lena" with different bit rates.

to recover horizontal boundaries. It is much different from those in the above two applications. When recovering vertical boundaries, the local window $\boldsymbol{l}$ is not a block any more, but a vector $\boldsymbol{l} = (l_{-4}, l_{-3}, l_{-2}, l_{-1}, l_0, l_1, l_2, l_3)$ of the pixel values across the boundary of two blocks in the blocky image, where $l_{-4}, l_{-3}, l_{-2}, l_{-1}$ and l_0, l_1, l_2, l_3 are two groups of pixels in the same line of the left and right blocks, respectively. The real block boundary is between x_{-1} and x_0. The remote window $\boldsymbol{r}$ also becomes a vector $\boldsymbol{r} = (r_{-4}, r_{-3}, r_{-2}, r_{-1}, r_0, r_1, r_2, r_3)$, but is a line of pixels within one block. We assume $\boldsymbol{r}$ is of good continuity and use the continuity of $\boldsymbol{r}$ to recover the discontinuity of $\boldsymbol{l}$. The search range is an m pixel wide and n pixel high rectangle region centered about the middle point of $\boldsymbol{r}$. The one-order linear function $v(z) = a_0 + a_1 z$ is used as the luminance transformation. The criterion for the evaluation of the matching result is also a modified version named weighted mean square error (WMSE)

$$\mathrm{WMSE} = \sum_{i=-4}^{3} w_i [l_i - v(r_i)]^2 = \sum_{i=-4}^{3} w_i [l_i - (a_0 + a_1 r_i)]^2 \tag{8}$$

where the weight vector $\boldsymbol{w} = (w_{-4}, w_{-3}, w_{-2}, w_{-1}, w_0, w_1, w_2, w_3)$ satisfies the following conditions: $0 \le w_i \le 1\ (i = -4, \ldots, 3), w_{-k} = w_{k-1}\ (k = 1, \ldots, 4)$ and $\sum_{i=-4}^{3} w_i = 1$. By solving the equations: $\partial \mathrm{WMSE}/\partial a_0 = 0$ and $\partial \mathrm{WMSE}/\partial a_1 = 0$, we can obtain the parameters

$$\begin{cases} a_1 = \dfrac{\sum_{i=-4}^{3} w_i l_i \cdot \sum_{i=-4}^{3} w_i r_i - \sum_{i=-4}^{3} w_i l_i r_i}{\left(\sum_{i=-4}^{3} w_i r_i\right)^2 - \sum_{i=-4}^{3} w_i r_i^2} \\ a_0 = \sum_{i=-4}^{3} w_i l_i - a_1 \cdot \sum_{i=-4}^{3} w_i r_i \end{cases} \tag{9}$$

The remote window with the minimal WMSE is the winner. In the recovered local vector $\boldsymbol{l}^{(\mathrm{new})} = (l_{-4}^{(\mathrm{new})}, l_{-3}^{(\mathrm{new})}, \ldots, l_3^{(\mathrm{new})})$, Each $l_i^{(\mathrm{new})}$ is a linear combination of l_i and $v(r_i)$

$$l_i^{(\mathrm{new})} = [1 - c_i \cdot g(\mathrm{WMSE})] \cdot l_i + c_i \cdot g(\mathrm{WMSE}) \cdot v(r_i) \tag{10}$$

where the vector $\boldsymbol{c} = (c_{-4}, c_{-3}, c_{-2}, c_{-1}, c_0, c_1, c_2, c_3)$ is selected so that $0 \le c_i \le 1\ (i = -4, \ldots, 3)$ and $c_{-k} = c_{k-1}\ (k = 1, \ldots, 4)$. $g(\mathrm{WMSE})$ is defined as

$$g(\mathrm{WMSE}) = \begin{cases} 1 - \left(\frac{1 - T_C}{T_E}\right) \cdot \mathrm{WMSE}, & \text{if } 0 \le \mathrm{WMSE} \le T_E \\ 0, & \text{otherwise} \end{cases} \tag{11}$$

where T_C and T_E are two parameters used to control the shape of $g(\mathrm{WMSE})$. The goal of using $\boldsymbol{c}$ and $g(\mathrm{WMSE})$ is to provide a tradeoff between modification and maintenance of $\boldsymbol{l}$. $\boldsymbol{c}$ should be chosen so that the closer the pixel is to the block boundary, the more it is modified. $g(\mathrm{WMSE})$ is selected so that the better $\boldsymbol{r}$ can match $\boldsymbol{l}$, the more $\boldsymbol{l}$ is modified.

In our experiments, the test images are first coded using JPEG standard at different bit rates ranging from about 0.15 to 0.45-bpp. The JPEG decoded images are then subject to our blocking effect reduction algorithm. The following control parameters are chosen: $m = 64, n = 32$ for vertical block boundaries and $m = 32, n = 64$ for horizontal block boundaries, respectively; $T_E = 200; T_C = 0.75; \boldsymbol{w} = (0.2, 0.15, 0.1, 0.05, 0.05, 0.1, 0.15, 0.2)$; and $\boldsymbol{c} = (0.25, 0.55, 0.65, 1, 1, 0.65, 0.55, 0.25)$. The decoding and post-processing results of "Lena" image are shown in Fig. 8. By using our blocking effect reduction algorithm, PSNR's are improved by a magnitude of 0.2 dB–0.85 dB. Our algorithm achieves relatively good results among those obtained by other approaches such as POCS [22], CLS [22], and Crouse *et al.*'s method [23], which are also shown in Fig. 8. Fig. 9 gives subjective illustrations of the decoding and post-processing results of the enlarged hat region of "Lena". The quality of the post-processed image is enhanced when compared with the JPEG-decoded image.

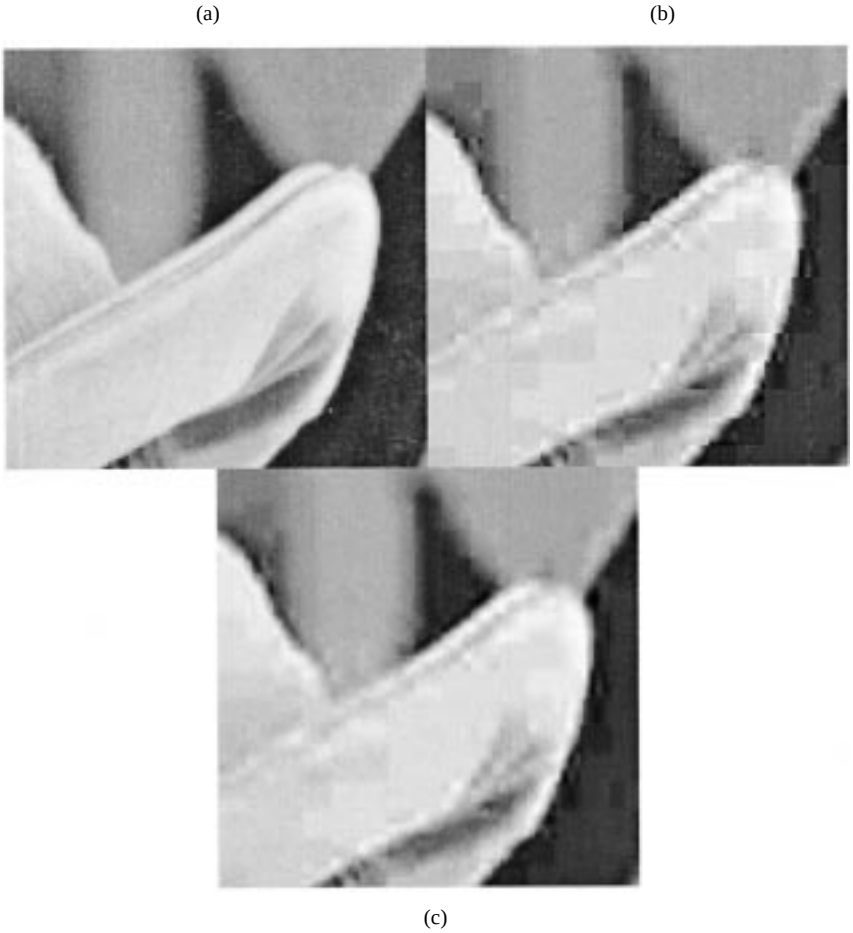

Fig. 9. Illustration of post-processing result for hat region of "Lena." (a) Original image. (b) JPEG-decoded image. (c) Post-processed image.

IV. Discussion and Extension

The basic concept of the general long-range correlation based approach is very flexible in real applications. Many concrete algorithms can be derived from it.

First, the local window l can be of any shape. Usually, square blocks are the most convenient, but in some cases, such as for blocking effect reduction, using other shapes may become better. Different shapes of local windows can also be used in dealing with one image.

Second, the searching for a remote window can be conducted by many different ways. The goal is to find the best matching of the local window in the least time. Fig. 10 shows a statistical result in percentage on a remote-local window distance in BNM error-concealment algorithm for two cases. In the first case, the remote blocks are randomly selected from the search range, while in the other case, the remote blocks are found by the BNM algorithm. It appears that the remote windows with shorter distance from the local window are more likely to be chosen by the BNM algorithm. According to such statistical characteristics, many intelligent methods can be used to improve the searching speed. For example, we can search for the best remote window by way of a spiral route starting from the center local window, so that the shorter the distance between the candidate remote window and the local window, the earlier it is searched. In the usage of this searching method, no search range restriction is needed. The searching procedure can stop once we find a satisfactory remote window. Some random searching method, such as the evolutionary strategy-based method, may also be used for fast searching.

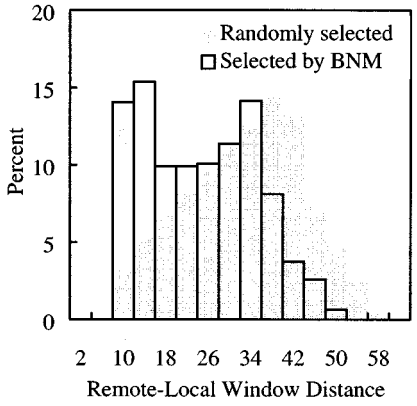

Fig. 10. Statistics on randomly selected and BNM selected remote-local window distances. The data are obtained from the test where "Barb" is corrupted with isolated block losses and with a block loss rate of 10%.

Third, there may be many different matching methods. In the algorithms introduced above, only direct matching and polynomial matching methods are used. In fact, other kinds of luminance transformations—including nonlinear transformations—can also be employed. Since the neural network models

are very good at establishing relationships between two sets of complex data, they may also be considered as substitutes of the matching functions. Another possible modification is to use an adaptive method to automatically select a luminance transformation function from many different kinds of matching functions. As a result, the merits of different matching methods may be combined.

Next, more complex matching evaluation and competition standards can be considered. Usually, MSE_M is used, but the mean absolute error in the matching part (MAE_M) between the local and the transformed remote widow can also be employed. In the blocking-effect reduction algorithm, we are using WMSE. Since the best remote window is more likely to appear in the near region in accordance with the statistics in Fig. 10, we can also combine the remote-local window distance as one of the factors for competition, so that the nearer remote window becomes more likely to be chosen. A possible further improvement is to combine all these factors together with different weights. In [26], we used a fuzzy matching evaluation method that is combined with a pre-applied fuzzy impulse detection algorithm. This fuzzy method is very effective in dealing with "vague" data.

Finally, the recovering method may also be improved. Actually, the recovering technique in the blocking effect reduction algorithm, where the pixel values from the transformed remote window and those in the original local window are combined, is a good example of an improved recovery method. This combination improves the image quality without the loss of any useful information. In [26], a fuzzy recovery method is used, so that the more a pixel looks like a damaged pixel, the more it is modified. This technique is powerful in eliminating random-valued impulse noises in the images because in this kind of noisy image, many damaged pixels are difficult to be definitely determined as impulses. We list our restoration results for "Lena" image at the last row of Table II. Although the result for the removal of fixed-valued impulses is not as good as our basic long-range correlation method, the result for random-valued impulsive noises appears to be a major improvement.

V. Conclusion

In this paper, we show that abundant long-range correlation exists within natural images, and that the human visual systems composed of our eyes and brains can sufficiently utilize such types of information redundancy to implement the functions of image interpretation, representation, restoration, enhancement, and error concealment. Furthermore, a practical general image-restoration and error-concealment algorithm using such long-range correlation is provided. Experimental results in several real applications show that the algorithm is very effective and provides a significant improvement over traditional techniques. Our approach can be further improved and extended in many ways and is very flexible for practical applications. The use of long-range information within the same image allows our approach to be completely free from any pre-assumption on the structure or spectra of the local regions. This is also a major difference in comparison with the traditional methods. In conclusion, our approach is an inherently intelligent and adaptive algorithm.

References

[1] G. A. Baxes, *Digital Image Processing: Principles and Applications*. New York: Wiley, 1994.

[2] A. Jacquin, "Image coding based on a fractal theory of iterated contractive image transformation," *IEEE Trans. Image Processing*, vol. 1, pp. 18–30, Jan. 1992.

[3] Y. Fisher, Ed., *Fractal Image Compression—Theory and Applications*. New York: Spring-Verlag, 1994.

[4] G. Walleye, "The JPEG still image picture compression standard," *Commun. ACM*, vol. 34, no. 4, pp. 30–44, Apr. 1991.

[5] D. Le Gall, "MPEG: A video compression standard for multimedia applications," *Commun. ACM*, vol. 34, no. 4, pp. 46–58, Apr. 1991.

[6] M. Liou, "Overview of the $p \times 64$ kbit/s video coding standard," *Commun. ACM*, vol. 34, no. 4, pp. 59–63, Apr. 1991.

[7] Y. Wang and Q. Zhu, "Signal loss recovery in DCT-based image and video codecs," *Proc. SPIE Vis. Commun. Image Processing*, vol. 1605, pp. 667–678, Nov. 1991.

[8] H. Sun, K. Challapali, and J. Zdepski, "Error concealment in digital simulcast AD-HDTV decoder," *IEEE Trans. Consumer Electron.*, vol. 38, pp. 108–118, Aug. 1992.

[9] W. M. Lam and A. R. Reibman, "An error concealment algorithm for image subject to channel errors," *IEEE Trans. Image Processing*, vol. 4, pp. 533–542, May 1995.

[10] X. Lee, Y. Q. Zhang, and A. Leon-Garcia, "Information loss recovery for block-based image coding techniques—A fuzzy logic approach," *IEEE Trans. Image Processing*, vol. 4, pp. 259–273, Mar. 1995.

[11] H. Sun and W. Kwok, "Concealment of damaged block transform coded images using projections onto convex sets," *IEEE Trans. Image Processing*, vol. 4, pp. 470–477, Apr. 1995.

[12] S. S. Hemami and T. H. Y. Meng, "Transform coded image reconstruction exploiting interblock correlation," *IEEE Trans. Image Processing*, vol. 4, pp. 1023–1027, July 1995.

[13] H. M. Lin and A. N. Willson, "Median filters with adaptive length," *IEEE Trans. Circuits Syst.*, vol. 35, pp. 675–690, June 1988.

[14] R. C. Hardie and K. E. Barner, "Rank conditioned rank selection filters for signal restoration," *IEEE Trans. Image Processing*, vol. 3, pp. 192–206, Mar. 1994.

[15] T. Sun and Y. Neuvo, "Detail-preserving median based filters in image processing," *Pattern Recognit. Lett.*, vol. 15, pp. 341–347, 1994.

[16] E. Abreu, M. Lightstone, S. K. Mitra, and K. Arakawa, "A new efficient approach for the removal of impulse noise from highly corrupted images," *IEEE Trans. Image Processing*, vol. 5, pp. 1012–1025, June 1996.

[17] D. Zhang and Z. Wang, "Impulse noise removal using polynomial approximation," *Opt. Eng.* , vol. 37, no. 4, 1998.

[18] Z. Wang and D. Zhang, "Restoration of impulse noise corrupted images using long-range correlation," *IEEE Signal Processing Lett.*, vol. 5, pp. 5–8, 1998.

[19] H. C. Reeve III and J. S. Lim, "Reduction of blocking artifacts in image coding," *Opt. Eng.*, vol. 23, no. 1, pp. 34–37, Jan./Feb. 1984.

[20] H. S. Malvar and D. H. Staelin, "The LOT: Transform coding without blocking effects," *IEEE Trans. Acoust., Speech, Signal Processing*, vol. 37, pp. 553–559, 1989.

[21] A. Zakhor, "Iterative procedures for reduction of blocking effects in transform image coding," *IEEE Trans. Circuits Syst. Video Technol.*, vol. 2, pp. 91–95, Mar. 1992.

[22] Y. Yang, N. P. Galatsanos, and A. K. Katsaggelos, "Regularized reconstruction to reduce blocking artifacts of block discrete cosine transform compressed images," *IEEE Trans. Circuits Syst. Video Technol.*, vol. 3, pp. 421–432, Dec. 1993.

[23] M. Crouse and K. Ramchandran, "Nonlinear constrained least squares estimation to reduce artifacts in block transform-coded images," in *Proc. ICIP '95*, vol. 1, Oct. 1995, pp. 462–465.

[24] Y. Q. Zhang, R. L. Pickholtz, and M. H. Loew, "A new approach to reduce the "blocking effect" of transform coding," *IEEE Trans. Communications*, vol. 41, pp. 299–302, Feb. 1993.

[25] J. Luo, C. W. Chen, K. J. Parker, and T. S. Huang, "Artifact reduction in low bit rate DCT-based image compression," *IEEE Trans. Image Processing*, vol. 5, pp. 1363–1368, Sept. 1996.

[26] D. Zhang and Z. Wang, "Impulse noise detection and removal using fuzzy techniques," *Electron. Lett.*, vol. 33, no. 5, pp. 378–379, 1997.

David Zhang (S'90–M'92–SM'95) received the B.S. degree in computer science from Peking University, Peking, China, and the M.Sc. and Ph.D. degrees in computer science and engineering from Harbin Institute of Technology (HIT), Harbin, China, in 1983 and 1985, respectively. He received his second Ph.D. degree in electrical and computer engineering from the University of Waterloo, ON, Canada, in 1994.

From 1986 to 1988, he was a post-doctoral Fellow at Tsinghua University, Beijing, China, and became an Associate Professor at Academia Sinica, Beijing, China. In 1988, he joined the University of Windsor, ON, Canada, as a Visiting Research Fellow in Electrical Engineering. After that, he was an Associate Professor with the City University of Hong Kong. Currently, he is a Professor with Hong Kong Polytechnic University, Kowloon, Hong Kong. He is Founder and Director of both Biometrics Technology Centres, supported by UGC/CRC, the Hong Kong Government, and the National Nature Scientific Foundation (NSFC) of China, respectively. He is also a Guest Professor at Tsinghua University, Shanghai Jiao Tong University, and HIT. To date, he has published over 170 papers, including seven books, in his areas of research.

Dr. Zhang is an Associate Editor for the IEEE TRANSACTIONS ON SYSTEMS, MAN, AND CYBERNETICS, *Pattern Recognition*, the *International Journal of Pattern Recognition and Artificial Intelligence*, *International Journal of Robotics and Automation*, and *Neural, Parallel and Scientific Computations*. He is also is Founder and Editor-in-Chief *International Journal of Image and Graphics*. He has given many keynotes, invited talks, and tutorial lectures, as well as served many times as a program/organizing committee member at international conferences in recent years.

Zhou Wang received the B.S. degree from Huazhong University of Science and Technology, Huazhong, China, in 1993, the M.S. degree from South China University of Technology, Guangzhou, China, in 1995, and the Ph.D. degree from the The University of Texas at Austin in 2001.

Since 1998, he has been a Research Assistant at the Laboratory for Image and Video Engineering, Department of Electrical and Computer Engineering, the University of Texas at Austin. During the summers of 2000 and 2001, he was with the Multimedia Technologies Department at IBM T. J. Watson Research Center, Yorktown Heights, NY. From 1996 to 1998, he was a Research and Teaching assistant at the Department of Computer Science, City University of Hong Kong, Hong Kong, China. His current research interests include image and video processing, coding, communication, and quality assessment, computer vision, pattern recognition, wavelets, fractals, fuzzy technologies, and artificial neural networks.